

DOE/BC/15211-10
(OSTI ID: 773827)

A PORE-NETWORK MODEL OF IN-SITU COMBUSTION IN POROUS
MEDIA

Topical Report
January 2001

By
Chuan Lu
Yanis C. Yortsos

Date Published: January 2001

Work Performed Under Contract No. DE-AC26-99BC15211

University of Southern California
Los Angeles, California



National Petroleum Technology Office
U.S. DEPARTMENT OF ENERGY
Tulsa, Oklahoma

DISCLAIMER

This report was prepared as an account of work sponsored by an agency of the United States Government. Neither the United States Government nor any agency thereof, nor any of their employees, makes any warranty, expressed or implied, or assumes any legal liability or responsibility for the accuracy, completeness, or usefulness of any information, apparatus, product, or process disclosed, or represents that its use would not infringe privately owned rights. Reference herein to any specific commercial product, process, or service by trade name, trademark, manufacturer, or otherwise does not necessarily constitute or imply its endorsement, recommendation, or favoring by the United States Government or any agency thereof. The views and opinions of authors expressed herein do not necessarily state or reflect those of the United States Government.

This report has been reproduced directly from the best available copy.

DOE/BC/15211-10
Distribution Category UC-122

A Pore-Network Model of In-Situ Combustion in Porous Media

By
Chuan Lu
Yanis C. Yortsos

January 2001

DE-AC26-99BC15211

Prepared for
U.S. Department of Energy
Assistant Secretary for Fossil Energy

Tom Reid, Project Manager
National Petroleum Technology Office
P.O. Box 3628
Tulsa, OK 74101

Prepared by
Department of Chemical Engineering
University of Southern California
University Park Campus
HEDCO 316, USC
Los Angeles, CA 90089-1211

TABLE OF CONTENTS

Abstract	v
Introduction	1
Pore-Network Model and Numerical Method	5
Results and Discussion	11
Concluding Remarks.....	18
References	21
Table 1	25
Figures 1-11	26-31

ABSTRACT

In-situ combustion in porous media find applications in a variety of problems. Existing models to date are based on a continuum description, in which effective porous media are used. In this report, we consider the use of dual pore networks (pores and solid sites) for modeling the effect of the microstructure on combustion processes in porous media. The model accounts for flow and transport of the gas phase in the porespace, where convection predominates, and for heat transfer by conduction in the solid phase. Gas phase flow in the pores and throats is governed by Darcy's law. Heterogeneous combustion with one-step finite kinetics is assumed at the pore walls. The time-dependent problem is solved numerically using a fully implicit scheme. The validity of the model is tested against existing 1-D solutions, in which three types of combustion patterns arise, depending on the value of a dimensionless parameter related to the ratio of heat capacities. Then, we report on 2-D simulations for forward combustion. The development of sustained front propagation is studied as a function of various parameters, which include heat losses, instabilities, a correlated porespace and the distribution of fuel. Implications of the findings for continuum models are discussed.

INTRODUCTION

In-situ combustion (ISC) is a well-known process for the recovery of heavy oil from oil reservoirs. Extensive reviews of the method and its field applications have been provided in the literature (Prats, 1982). Even though one of the oldest techniques for heavy oil recovery, however, ISC is also one of the most complex. In addition to the common mechanisms it shares with conventional recovery methods, such as waterflooding and steamflooding, ISC involves the additional complexity of the oxidation reactions. These serve to, first, form the fuel in a regime of Low Temperature Oxidation (LTO) and, subsequently, provide the main combustion reaction under conditions of High Temperature Oxidation (HTO). The main goal of ISC is the sustained propagation of combustion fronts, to supply the necessary heat for viscosity reduction and the self-sustaining of the overall process. As a result, issues of front stability, sustained front propagation and possible extinction are of fundamental importance.

A large number of studies have been published in the literature on ISC, addressing a wide range of issues, from the detailed kinetics of the reaction processes to mathematical models to field applications. Of specific interest to this study is the modeling of the combustion process. Typically, this is done using conventional continuum models, in which reaction rates, concentrations and temperatures are volume-averaged continuum variables. The solution of such models is then sought in the various applications of interest, including laboratory and field scales. This approach has validity as long as the following conditions hold: that the variables of interest, such as concentrations, temperature and reaction rates, do not involve large gradients in space at the underlying microscale, for volume-averaged quantities to be meaningful; and that the effective parameters used in the continuum models reflect fairly accurately the actual processes. Because of the strong non-linearities involved in reaction kinetics, particularly of the Arrhenius dependence of the true reaction rate on temperature,

$$r \propto C \exp\left(-\frac{E}{RT}\right)$$

the volume average of the rate will not have the same dependence, namely

$$\langle r \rangle \neq \langle C \rangle \exp\left(-\frac{E}{R \langle T \rangle}\right)$$

if the local concentration or temperature vary significantly over the averaging volume.

Large gradients at the microscale may occur for a number of reasons. The development of sharp propagating fronts is one of them. In displacement processes, fronts arise naturally, due to the different characteristic velocities of the initial and the injected states (a classical example of which is the shock front in a Buckley-Leverett type displacement). The thickness of such fronts is controlled by dissipation, like diffusion, capillarity and conduction. For the case of ISC, however, sharp fronts also result from the fast kinetics of the combustion reactions in the HTO region and the depletion of some of the various chemicals that participate in the reaction. The resulting reaction zones are thin, and give rise to large gradients within the microstructure. The possible development of spatial instabilities is another important cause of large gradients.

The second concern is, in general, the effect on the overall process of small-scale heterogeneities of fluid flow, mass and heat transfer, and chemical reactivity. Local heterogeneities arise due to the randomness of the microstructure, and may result in a distribution of the local variables that can affect the volume-averaged rates as noted above. In addition, of importance to sustained propagation and extinction is the spatial distribution of the fuel in the pores of the microstructure. If the fuel is sparsely distributed, the sustained spreading of combustion across the pore network requires certain conditions on the rates of reaction, heat and mass transfer. Otherwise, the process will become extinct. For problems in which sustained propagation or extinction are critical issues,

having an accurate assessment of the phenomena at the microscale becomes then an important objective. This is possible with the development of a pore-network model of ISC, which forms the objective of this study.

As is well known, there are several distinct regions during an ISC process (Prats, 1982, Boberg, 1988). From the injection well, they are the swept region, the combustion/cracking zone, the vaporization and LTO zone, the steam zone, the hot water bank, the oil bank and the initial zone (see schematic of Figure 1). For simplicity and by necessity, in this paper we will focus on the HTO regime and ignore the other downstream regimes. Thus, the problem to be modeled is the combustion of a solid fuel, deposited in the porespace, by the injection of a gas-phase oxidant. In a sense, the problem under consideration is similar to what is known as Filtration Combustion (FC) (Aldushin, 1993). The latter finds a variety of applications and has been analyzed in considerable detail in recent years, using continuum models. Some of these results will be reviewed below.

Pore-network models have been successfully used to model a variety of problems in porous media in the absence of reaction, from immiscible displacements to boiling (Lenormand et al., 1988, Blunt et al., 1991, Li and Yortsos, 1995, Satik and Yortsos, 1996). This has allowed for an accurate representation of effective parameters and for a better incorporation of small-scale mechanisms in continuum models. In processes involving reactions, applications of pore networks have been mainly in the areas of heterogeneous reactions on catalysts, catalysts deactivation, acidization, dissolution of trapped pollutants, etc. [8-11]. Discrete models for FC, and more specifically for ISC processes, have not appeared in the literature to our knowledge (see also below). This report attempts to fill this gap. The approach to be implemented is analogous to an earlier effort to model thermal processes at the pore-network scale, for example in heat-

transfer driven bubble growth. The important difference is that here the exothermic combustion reaction at the pore surface must also be included.

Before proceeding, we need to mention that similarities exist between ISC and the process of self-propagating high temperature synthesis (SHS) for the development of new materials (Hwang et al., 1997, 1998). The difference is that in the latter process, the reaction rate depends only on temperature and not on gas-phase concentrations. Experimental investigations have provided much information concerning SHS processes. An understanding of the microscopic processes is crucial to predicting the microstructure and properties of the final product. A numerical model akin to a pore-network model was developed by Hwang et al. (1998), based on which they were able to simulate effects of heterogeneity on the conversion patterns, as a function of various parameters.

The model to be developed here is considerably more complex than that of Hwang et al. (1998). In addition to heat transfer, it accounts for the convection and diffusion of the injected oxidant, its chemical reaction with the fuel and the possible enhancement of permeability as a result of the HTO. Effects of heterogeneity in permeability, fuel distribution, and other variables are also included. The report is organized as follows: First, we describe the aspects of the pore-network model. Before we provide numerical simulation results, we also review some findings from continuum analyses of FC, in order to verify the validity of the model in special cases. Then, we provide numerical simulation results to examine the sensitivity of the system to various parameters. Finally, we discuss their implication regarding continuum models.

PORE-NETWORK MODEL AND NUMERICAL METHOD

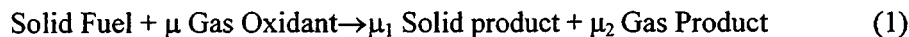
In this section, we describe the pore-network model and the numerical method used for its solution. Findings from the continuum model of FC are also discussed.

Model Description

The pore-network model consists of a dual network of pores and throats, which is embedded in a network of solid sites, representing the solid matrix (Figure 2). The pores (sites) are the places where reaction occurs and contain solid fuel of constant composition. They are interconnected via throats (bonds), which control transport of mass, momentum and heat, and which have distributed sizes. The network of solid sites is needed to account for heat transfer in the solid (e.g. see Satik and Yortsos, 1996). The coupling of solid and pore-space occurs through the heat transfer between pores and solid sites as shown in Figure 2.

In the 2-D simulations to be reported below, both networks are square lattices, of an adjustable length and width. The features on mass and heat transport include the following:

1. In 2-D, each solid site communicates with 4 solid sites (shown in Figure 2a by the thin solid line between solid sites) and 1 pore site (the dash line between solid and pore sites), through heat conduction. A heat transfer coefficient is used to model the pore-solid exchange.
2. Injection of a mixture of oxidant and inert gas occurs at one end, where pressure, temperature and composition are specified. The outlet end is at a constant pressure to maintain the injection rate. Flow in the pore throats is governed by Poiseuille's law. The oxidant in the gas phase is delivered by gas-phase diffusion and convection.
3. The following heterogeneous reaction is assumed,



where μ , μ_1 , and μ_2 are the stoichiometric coefficients. Implicit in the above is the assumption that the reaction is heterogeneous and does not involve the propagation of flame in the pore network. The reaction rate is expressed by the one-step kinetic model

$$R = k_r A_r P X_o H(V_f) \exp\left(-\frac{E_a}{RT}\right) \quad (2)$$

where H is the step function, V_f is the volume of fuel, P is the total pressure, k_r is the kinetic constant, A_r is the interface area in an individual pore site, X_o the mass fraction of the oxidant and E_a the activation energy. More complex kinetics, including multi-step, parallel or serial schemes, could also be adopted.

4. Within a pore site, thermodynamic equilibrium is assumed, such that concentrations, pressure and temperature are uniform. This also implies that fuel and gas are at thermal equilibrium. However, heat transfer does take place between adjacent pore sites, between pore and solid sites and between adjacent solid sites. Though this configuration and our code allow for different thermodynamic and transport parameters, they are taken constant to avoid extra complexity. Variables assigned to sites and bonds are listed in Table 1.

Governing Equations

The governing equations for FC have been developed for some time now. Due to the multi-phase nature of the process, they must be able to account separately for the properties of the different phases and to also describe their interaction mechanisms. Ohlemiller (1986) provided a formalism that includes single particle/bulk condensed phase equations, to describe the behavior of the solid phase temperature and mass balance, and bulk gas equations, to determine the temperature, concentration, pressure and velocity profiles in the gas phase. Currently, most models of the FC processes adapt the bulk equations for both gas and condensed phases along with considerable other simplifications [15, 16].

Using appropriate mass and energy balances, we can write conservation equations for each site in the pore network, as follows:

Pore Site I, Adjacent to Pore-Site j:

Gas Phase Component k Mass Balance

$$\frac{\Delta(\frac{P_i V_i}{RT_i} y_{i,k} M_k)}{\Delta t} = -\sum_j u_{ij} r_y^2 \frac{P_i y_{i,k}}{RT_i} M_k - \frac{D_g}{lR} \sum_j r_y^2 \left(\frac{P_i + P_j}{2}\right) \left(\frac{2}{T_i + T_j}\right) (y_{i,k} - y_{j,k}) + \mu_k \left(k_r A_i' \frac{P_i y_{i,O_2}}{RT_i} \exp\left(-\frac{E_a}{RT_i}\right)\right) H(V_{i,f}) \quad (3)$$

Solid Fuel Conservation

$$\rho_f \frac{\Delta V_{i,f}}{\Delta t} = k_r A_i' \frac{P_i y_{i,O_2}}{RT_i} \exp\left(-\frac{E_a}{RT_i}\right) H(V_{i,f}) \quad (4)$$

Energy Balance

$$\frac{\Delta E_i}{\Delta t} = -\sum_j u_{ij} r_y^2 \frac{E_{g,i}}{V_i} - \frac{K_{gs}}{l} \sum_j r_y^2 (T_i - T_j) - h_s \sum_s A_{is}^h (T_i - T_s) - h_{L,p} A_{i,l}^h (T_i - T_0) \quad (5)$$

where, we defined the energy content of a site by

$$E_i = E_{f,i} + E_{g,i}$$

$$E_{f,i} = m_{f,i} (C_{p,f} T_i + \Delta_c H_f); E_{g,i} = \sum_k \frac{P_i V_i}{RT_i} M_k y_{i,k} (C_{pg,k} T_i + \Delta_c H_f) \quad (6)$$

Momentum Balance

$$u_{ij} = \frac{r_y^4}{8\mu l} (P_i - P_j) \quad (7)$$

Solid Site Energy Balance

$$\rho V C_{ps} \frac{\Delta T}{\Delta t} = -\frac{k_s^h}{l} \sum_{s'} A_{ss'}^h (T_s - T_{s'}) + h_s \sum_j A_{js}^h (T_j - T_s) - h_{L,S} A_{s,l}^h (T_s - T_0) \quad (8)$$

The sum in the energy balances express the heat exchange between pore and solid sites, while $h_{L,S}$ denotes heat loss to the surroundings. In addition, ideal gas behavior was assumed. Finally, the bond radius was correlated to the depth of conversion.

To make the equations dimensionless we introduce the characteristic values listed in Table 2. The corresponding dimensionless groups obtained are shown in Table 3. Together with other parameters, such as the initial temperature, the volume ratio of solid site to the pore site, the average initial fuel amount in pore sites and the oxidant concentration at injection, the dimensionless parameters constitute the main set of variables affecting the process.

Remarks

- The above model allows for simulating both forward and reverse combustion. These are differentiated by controlling the ignition point, which is the first row in the inlet for the case of forward combustion, and the row before the last in the outlet, for the reverse case (Figure 3). Our emphasis in this work is on forward combustion, although some brief comments on reverse combustion will also be made, where appropriate.
- Although the relation between flow rate and pressure difference depends on the Reynolds number, we will only assume laminar, Poiseuille flow. At the continuum level, this is equivalent to Darcy's law, an assumption which is very often made in the literature.
- Though radiation may play an important role because of the high temperature at the fronts, most analytical solutions and numerical simulations omit its effect. It was neglected in our model as well.
- As mentioned above, the kinetics of ISC are rather complicated. They can be accompanied by pyrolysis, evaporation and condensation, multi-step reactions and also by some gas-phase

reactions [3, 17, 18, 19]. However, in contrast to the well-developed flame kinetics, a detailed reaction mechanism for heterogeneous systems is still not widely used. Instead, one-step kinetics, as assumed above, is commonly accepted for the combustion of solid fuels.

- Finally, in our model, the heat released by the reactions is expressed in an implicit form. This differs from most previous works. The advantage of this formalism lies in the fact that one can ignore the detailed kinetics and the associated physical processes. The shortcomings are that it cannot describe processes at very high flow rates, which can break the thermal equilibrium between the gas phase and the fuel sites.

Numerical Method

The dimensionless equations were solved by standard implicit schemes. Because of the stiffness of the problem, time steps were confined to less than 1s. However, because the spatial scale needs to be large enough, it takes quite a long time to obtain reasonably accurate results. In previous works in homogeneous problems and stability investigations, adaptive pseudo-spectral algorithms have been applied (Bayliss and Matkowsky, 1987). Since the pore-network model has many features in common with a discretization scheme, we can assign transport properties, either by making the scheme 2nd order accurate or of an upwind character. In our calculations, it was found that numerical dispersion affects the results only when the injection rate is sufficiently high ($Pe \gg O(1)$). For such cases, special methods were adopted. An implicit predictor-corrector method was employed for the temporal evolution. This method is 2nd order accurate in most cases.

In order to speed up the computations, further simplifications were necessary. To this effect, we introduced the following assumptions:

1. Constant pressure

Since the gas viscosity is small, the pressure perturbation can be ignored in all governing equations, except in Poiseuille's law (Equation (7)). This assumption is based on the

condition that the flow rate is significantly smaller than the speed of sound, and is widely used in the simulations of laminar flames in open space. The computational advantages are that the momentum equation becomes decoupled, while the continuity equation is linearized.

2. Quasi-steady state in the gas phase

Because of the difference between the densities of gas and solid, the corresponding time scales are greatly different. Using dimensional analysis, Ohlemiller (1985) and Aldushin and Matkowsky (1998) pointed out that the transient gas terms can be neglected; then, the bulk gas as well as the gas within the condensed phase can be treated as quasi-steady.

Numerical simulation results showed that use of these assumptions dramatically decrease the computation time, without significant loss in accuracy in the pressure, temperature and concentration profiles.

In the general case, the equations are nonlinear and were solved by a Newton-Raphson method. A high-performance linear equations solver is needed. We have tried a traditional SOR method, a preprocessed conjugated gradient (PJCG) method and LSOR methods, which are effective for heterogeneous systems (where properties are different in different directions). The results show that at the beginning stage, the PJCG method converges faster. Then, the LSOR or the SOR methods have better performance. All of these three methods were used as appropriate. We must add that once a step diverges or the solid fuel depletes, the time step should be cut and integration must be repeated. This approach is similar to the PICO technique [22]. Instead of setting a constraint on the number of iteration times, however, we reduce the time step if convergence cannot be reached after 5 iterations in order to maintain accuracy. Although modified several times, and its performance sped up by more than 20 times, the computational scheme is still time consuming. For 2-D cases, its accuracy and speed are acceptable. More effort on the optimization of the code is still needed, however, before it can be employed in 3-D simulations.

RESULTS AND DISCUSSION

In this section we present results from the numerical simulations. First, we test the validity of the model in some simple cases.

1-D Simulations

To test the validity of the pore-network model we first conducted 1-D simulations of forward combustion and compared the results with the analysis of Aldushin et al. (1999). These author

showed that the dimensionless parameter $\delta = \frac{c_g \mu \rho_{f0}}{C_s a_0}$ determines the condition for the existence

of three different structures, a reaction-leading pattern ($\delta > 1$), where the reaction front leads the thermal front, a reaction-trailing pattern ($\delta < 1$), where the reaction front trails the thermal front, and a wave with maximum energy accumulation ($\delta = 1$), in which the two fronts coincide and the

temperature at the front increases with time, according to the equation $T_b - T_0 = Q_A a_0 \sqrt{\frac{G_0 l}{\pi \lambda c_g}}$.

Our numerical results plotted in the left panel of Figure 4 are in good agreement with the theoretical predictions. In the first two cases, it is apparent that a traveling wave solution is rapidly reached, which propagates at a constant velocity. This velocity and the extent of the separation between fronts depend on a number of parameters, such as injection rate, heat conductivity, capacity, etc. Our model allows also to investigate the sensitivity of the results to heat losses. The right panel of Figure 4 shows the temperature profiles corresponding to the three cases, but with heat losses included. Although parameter δ appears to still remain the determining factor in the classification of patterns, the heat loss affects both the propagation velocity and the temperature patterns.

2-D Simulations: 1. Base case

We subsequently report on 2-D results using the base-case parameters listed in Table 4. We note that the porous medium has relatively large particles (the distance between pore sites is of the order of 0.5 mm), the fuel is uniformly partitioned in the pore sites, heat losses occur from the pore network to the surroundings at a rate which is 5% of the heat transfer rate between the gas and the solid, while the Peclet number for mass transfer is 0.05, for the relatively low injection rate used in the base case. The main local heterogeneity in the base state was on the pore throats, the size of which was randomly distributed. In addition, for the particular stoichiometry used, no net production or loss of moles in the gas phase can occur, namely the volumetric flux of the gas phase remains constant. The base case does not include a change of the pore throat size due to the fuel depletion. These have implications on the front stability, as will be discussed below.

For the values of the base state ($\delta < 1$), the pattern is reaction-leading. Typically, the basic structure consists of a leading reaction zone, where most of the combustion reaction occurs, the oxidant and the fuel are depleted fast, and the temperature rises sharply. This combustion front rapidly reaches a steady-state and propagates at constant velocity. Figure 5 shows typical simulation results for the fuel conversion depth, the temperature, the pressure (with respect to the pressure at the outlet end, and multiplied by a factor for illustration purposes) and the oxidant concentration. The extent of the reaction zone is estimated to be of the order of 1.5 mm, which in this case is equivalent to 3 pore lengths. This is consistent with estimates obtained from continuum calculations (Akkutlu and Yortsos, 2000). The profiles have some roughness, departing from strictly piston-like displacement, and temperature and concentrations (particularly the former) exhibit fluctuations. Averaging these fluctuations for use in continuum models would be an important consideration, as noted in the Introduction. However, there is no indication of fingering or instability in this base case. The pressure profiles indicate that the pressure varies

significantly near the combustion region, as a result of its high temperature. In addition, there is almost complete consumption of the injected oxidant at the front, thus there is no oxidant leakage across the front.

2-D Simulations: 2. Sensitivity Study

Using the base-case parameters, we next proceeded to a sensitivity study in order to assess the following effects: The possibility of extinction, instead of sustained propagation, the development of instabilities at the pore-network scale, the effect of spatially correlated pore-space and the effect of the distribution of the fuel in the pore network.

a. Extinction

The sustained front propagation was influenced mainly by the following factors: ignition, the oxidant concentration, the amount of heat losses and the fuel density. In all simulations, ignition was found necessary for the onset of the combustion reaction. For this, the temperature of the inlet row was raised to a sufficiently high value, while that of the adjacent row was also slightly raised (thus mimicking an initially sharp exponential profile) (see also Figure 3). Ignition was also found necessary for reverse combustion. In its absence or when the ignition temperature was low, the front quickly became extinct.

Extinction was also promoted by increased heat losses and decreased concentrations of the injected oxidant. For otherwise constant values of the base-case parameters, we found that extinction occurred if heat losses were increased to about 50% or higher of the rate of heat transfer between the porespace and the solid sites. For a more accurate determination of the threshold additional simulations are needed, however the onset of extinction as the rate of heat losses increases is consistent with continuum model predictions (Akkutlu and Yortsos, 2001).

These also suggest that for otherwise constant values, extinction can be circumvented by an increase in the injection rate. The effect of the injection rate is currently being studied. In addition, it was found that sustained front propagation is not possible if the mole fraction of the oxidant at the inlet is reduced to 28%. Again, this value is only indicative of a lower bound rather than a true threshold. It does indicate, however, that injection of a sufficiently rich mixture is required to sustain combustion. A detailed analysis is still in progress.

Before proceeding we show simulation results for the dependence of the front velocity on the injection rate for the base-case but in the absence of heat losses. As shown in Figure 6, the front velocity varies linearly with the injection rate and it is about two orders of magnitude smaller. The dependence in this region can be explained by simple mass balance arguments, given that both oxidant and fuel are completely consumed at the front. We note that in these simulations there is front propagation, even at very small injection rates, reflecting the fact that in this region combustion is promoted by diffusion only. However, it is unlikely that such a front will propagate further in an extended porous medium. We must also note that if the injection rate increases beyond the range shown in Figure 6, the front slows down.

b. Instabilities

From continuum analyses it is known that forward combustion fronts become stabilized by heat conduction, diffusion, and the net reduction in the number of gas moles due to the combustion reaction. They become destabilized by the net increase in the number of gas moles (expansion) and by an increase in the permeability of the burned region. As mentioned, in this work we only considered the case in which the net expansion is zero, an assumption which greatly facilitates computations. As a result, in the base case the fronts are stable (Figure 5), reflecting the stabilizing influence of conduction and diffusion. To investigate the onset of viscous fingering

instability we considered cases in which the pore throat radii of the burned region increase by a constant multiplier. We considered two cases in which the multiplier was 2 and 4, respectively. Given the use of Poiseuille's law, this translates into an effective increase of the permeability of the burned region by $2^4 = 16$, and $4^4 = 256$, respectively. Figure 7 shows the corresponding results for the second case. The effect of this rather substantial permeability contrast (which is analogous to a displacement with a mobility ratio of 256) is evident. The conversion depth acquires features of a viscous fingering pattern, the extent of reaction is non-uniform and the fluctuations of temperature and concentrations are substantial, despite the small size of the pore network. A distinct feature is that the corrugation of the front now gives rise to incomplete conversion in certain regions and a corresponding leakage of oxidant. This phenomenon was also observed when the pore structure was correlated (see below). Similar, but not as strong, effects were found in the case of the milder permeability contrast of 16.

The simulations in Figure 7 indicate that pore-network scale instabilities are possible provided that the permeability enhancement is sufficiently strong. While the level of such enhancement may be unrealistic, such instabilities will also develop when there is gas expansion at the front as a result of the combustion reaction. Our simulations cannot answer at present the question whether or not these instabilities at the pore-network scale will ultimately lead to process extinction. For their suppression requires a decrease of the injection rate, to promote the stabilizing effects of conduction and diffusion. A study of this effect is currently in progress. Such a decrease must not be too strong, however, since it may lead to extinction as a result of heat losses, as discussed above.

In passing, we must note that strong instabilities do develop in the case of reverse combustion. Now, diffusion is destabilizing, and at sufficiently small injection rates the developed pattern is unstable. For the sake of completeness we show in Figure 8 the results from a typical simulation

of reverse combustion. Patterns reminiscent of viscous fingering, including shielding, trapping and tip splitting are obtained. These patterns are accentuated as the injection rate decreases. An elaborate account of this problem will be presented elsewhere.

c. Correlated porespace

Sensitivity studies were subsequently conducted to investigate the effect of the pore-size distribution and its spatial correlation. First, we examined variations in the pore-size distribution.

Figure 9 shows results for the base case, but with the (uniform) pore-size distribution stretched so that the ratio of the end points increased from 3 (which is the base case) to 10. The simulations show that front roughness, reaction zone thickness and temperature and concentration fluctuations all increase. It is interesting to note, however, that there is no leakage of oxidant across the front. The effects shown in Figure 9 reflect the increased contrast in flow rates, hence in the convected flux of the gas oxidant, among the various pores. Subsequently, the effect of spatial correlations was investigated, by taking a pore-size distribution obeying fBm statistics (Du et al., 1996). These statistics reflect long-range correlations and, for the specific problem considered here, correspond to a correlation length equal to the network size. Corresponding results are shown in Figure 10 for a Hurst exponent $H=0.7$, which represents smooth fields with channel-like features. One effect of the correlated porespace is to increase the roughness of the front, as well as the fluctuations in temperature and concentrations. This is expected, due to the features of the correlated noise. What is important, in the correlated case, however, is that the gas oxidant is not completely consumed at the front. Rather, many regions develop at the front where the oxidant leaks through, partly unreacted (Figure 10). The incomplete combustion is a rather striking effect of the spatial correlation and was observed also in other simulations. The fact that the underlying pore structure influences the pattern to be developed is shown in Figure 11, for the case of a

“microfissure” in the porespace. In these simulations, one row in the pore-network has a uniform pore-size distribution the end points of which were four times larger than in the rest. The results of Figure 11 correspond to an injection rate 10 times larger than in the base case. With this rate, the process becomes convection-controlled and the patterns reflect clearly the underlying features of the pore-space. The process is similar to the displacement of one fluid by another in a fractured medium. Whether or not this pattern will persist for a long time, however, cannot be answered by the pore-scale simulations, and must be addressed by different means. We must note that by decreasing the injection rate, the “imprint” of the microstructure on the combustion pattern waned, as expected.

d. Distribution of fuel

The final effect studied in the sensitivity analyses was the distribution of fuel in the porespace. The issue that arises is the following. Assume that the fuel is randomly distributed in the sites of the pore-network, namely that there is a probability p that a site contains fuel. The question is whether there exists a critical value (a percolation threshold) p_c , above which sustained propagation is possible, but below which extinction occurs. It is clear that this value will depend on a number of parameters, an important one being the thermal conductivity of the solid. The role of the latter is not trivial: If conductivity is small, then the sustained propagation of combustion requires that fuel sites, which here act as a heat source, are sufficiently close, hence that p_c is large. In that region, we expect that as the thermal conductivity increases, then p_c will decrease. However, as the thermal conductivity is sufficiently large it is possible that the heat generated spreads out more than needed resulting in the extinction of the process, unless p_c increases. Results from simulations are shown in the graph of Figure 12. Consistent with the above, the curve of p_c vs. thermal conductivity is non-monotonic. At low values of the thermal conductivity the percolation threshold is a decreasing function, then reaches a relatively flat plateau, and

subsequently increases with further increase in thermal conductivity. It is interesting to note that in this process values larger than the typical percolation threshold of 0.59 for site percolation in a square lattice can be obtained. The results of such simulations suggest that the volume-averaged fraction of fuel per unit volume must exceed a critical value for the sustained propagation of a combustion front. This critical value reflects not only intrinsic thermodynamic and kinetic properties, but also the spatial arrangement of the fuel in the porespace.

CONCLUDING REMARKS

In this report we developed a pore-network model to simulate the High Temperature Oxidation region of in-situ combustion in porous media. The pore-network model is based on dual pore networks (pores and solid sites) and has the objective to incorporate the effect of microstructure on combustion processes in porous media. The model accounts for flow and transport of the gas phase in the porespace, where convection predominates, and for heat transfer by conduction in the solid phase. Gas phase flow in the pores and throats is assumed to be governed by viscous forces. Heterogeneous combustion with one-step finite kinetics was assumed. The validity of the model was tested against existing 1-D solutions. A variety of 2-D simulations were conducted to investigate the effects of parameters. In particular, we focused on the patterns of the extent of conversion, temperature, pressure and oxidant concentration.

In the absence of gas phase expansion at the front, the combustion fronts are found to be generally stable and of a finite degree of roughness. The latter increases with a more broad pore-size distribution and with spatially correlated pores. In the base case, both fuel and oxidant are fully consumed within a thin reaction zone, the thickness of which does not exceed a few pore lengths. When spatial correlations occur, however, the oxidant leaks through the front, along the

correlated pathways. The development of sustained front propagation was studied as a function of various parameters, which included heat losses, instabilities, and the distribution of fuel. Particular attention was paid to the latter, where it was found that the geometric distribution of the fuel in the pore sites is also a parameter that affects the extinction boundaries. The problem can be posed as an extended percolation like process from which percolation-like thresholds can be computed.

The implications of the study to the validity and the application of continuum models are many-fold. Even in the absence of 2-D effects, the pore-network study shows that the HTO zone is very thin and of the order of a few pore lengths, a fact that makes the application of continuum models questionable, given that the latter presume the absence of gradients over the volume of averaging (which is of the order of hundreds of pores). When 2-D and 3-D effects are included, fronts additionally show roughness, instabilities or non-uniform properties. Existing continuum models, based on a direct extrapolation of intrinsic kinetics to the continuum scale, do not account for many of these effects. Salvaging the continuum description can be obtained by incorporating the findings at the pore-network scale. One such method would be to derive effective kinetic parameters, such as rate constants and activation energies, by matching the steady-state predictions from continuum and pore-network models. Such a study is currently underway. The results for the effect of the spatial fuel distribution on the sustained propagation of combustion fronts should also be incorporated in continuum models, as the latter are intrinsically incapable for such an account.

REFERENCES

1. Prats, M., *Thermal Recovery*, SPE Monograph Series SPE of AIME (1982).
2. Boberg, T.C., *Thermal Methods of Oil Recovery*, An Exxon Monograph Series (1988).
3. Aldushin, A.P., *New results in the theory of filtration combustion*, COMBUSTION AND FLAME 94: 308-320 (1993).
4. Lenormand, R., Touboule, C. and Zarcone, C., *Numerical Models and Experiments on Immiscible Displacements in Porous Media*, J. FLUID MECH. 189: 165 (1988).
5. Blunt, M., and King, P., *Relative Permeabilities from Two- and Three-Dimensional Pore-Scale Network Modeling*, Transp. Porous Media 6, 407-433 (1991).
6. Li, X., and Yortsos, Y.C., *Visualization and Simulation of Bubble Growth in Pore Networks*, AIChEJ 41, 214 (1995).
7. Satik, C., and Yortsos, Y.C., *A Pore-Network Study of Bubble Growth in Porous Media Driven by Heat Transfer*, J. HEAT TRANSFER 118, 455-462 (1996).
8. Andrade, J.S., Street, D.A., Stanley, H.E., *Diffusion and Reaction in Percolating Pore Networks*, PHYS. REV. E 55, 772-777 (1997).
9. Rieckmann, C., and Keil, F.J., *Multicomponent diffusion and reaction in three-dimensional networks: general kinetics*, IND. ENGNG. CHEM. RES. 36, 3275 (1997).
10. El-Nafaty, U.A., and Mann, R., *Support-pore architecture optimization in FCC catalyst particles using designed pore networks*, CHEM. ENG. SCI. 54, 3475-3484 (1999).
11. Jia, C., Shing, K. and Yortsos, Y.C., *Visualization and Simulation of Non-Aqueous Phase Liquids Solubilization in Pore Networks*, J. CONTAM. HYDR., 35, 363 (1999).
12. Hwang, S., Mukasyan, A.S., Rogachev, A.V., and Varma, A., *Combustion wave microstructure in gas solid reaction systems: experiments and theory*, COMBUST. SCI. AND TECH. 123, 165 (1997).

13. Hwang, S., Mukasyan, A.S., and Varma, A., *Mechanisms of combustion wave propagation in heterogeneous reaction systems*, COMBUST. AND FLAME 115, 354-363 (1998).
14. Ohlemiller, T.J., *Modeling of smoldering combustion propagation*, PROG. ENERGY COMBST. SCI. 11, 277-310 (1985).
15. Henneke, M.R., and Ellzey, J.L., *Modeling of filtration combustion in a packed bed*, COMBUSTION AND FLAME 117, 832 (1999).
16. Goldfarb, I., Gol'dshtein, V., Kuzmenko, G., and Sazhin, S., *Thermal radiation effect on thermal explosion in gas containing fuel droplets*, COMBUSTION THEORY AND MODELLING 3, 769-787 (1999).
17. Summerfield, M., Ohlemiller, T.J., Sandusky, H.W., *A thermophysical mathematical model of steady-draw smoking and predictions of overall cigatte behavior*, COMBUSTION AND FLAME 33, 263-279 (1978).
18. Kisler, J.P., and Shallcross, D.C., *An improved model for the oxidation processes of light crude oil*, Trans IchemE 75A, 392-400 (1997).
19. Leach, S.V., Rein, S., Ellzey, J.L., Ezekoye, O.A., and Torero, J.L., *Kinetics and fuel property effects on forward smoldering*, COMBUSTION AND FLAME 120, 346-358 (2000).
20. Bayliss, A., and Matkowsky, B.J., *Fronts, relaxation oscillations, and period doubling in solid fuel combustion*, J. COMPUTATIONAL PHISICS 71, 147-168 (1987).
21. Aldushin, A.P., and Matkowsky, B.J., *Instabilities, fingering and the Saffman-Taylor problem in filtration combustion*, COMBUST. SCI. TECHN. 133, 293-341 (1998).
22. Issa, R.I., Gosman, A.D., and Ahmadi-Befrui, B., *Solution of the implicitly discretised reacting flow equations by operator splitting*, J.COMPUT. PHYS. 93, 388-410 (1991).
23. Aldushin, A.P., Rumanov, I.E., and Matkowsky, B.J., *Maximal energy accumulation in a superadiabatic filtration combustion wave*, COMBUSTION AND FLAME 118, 17-90 (1999).

24. Akkutlu, I.Y., and Yortsos, Y.C., *The Dynamics of Combustion Fronts in Porous Media*, paper SPE 63225, presented at the 2000 SPE Fall Meeting, Dallas, Tx (Oct. 2000).
25. Akkutlu, I.Y., and Yortsos, Y.C., in preparation (2001).
26. Du, C., Satik, G., and Yortsos, Y.C., *Percolation in a Fractional Brownian Motion Lattice*, AICHEJ 42, 2392-2395 (1996).

Table 1. Variables Assigned to Sites and Bonds

Pore Site Properties	Solid Site Properties	Bond Properties
Void volume	Volume	Length*
Interface area for reaction	Heat transfer area between solid sites	Radius
Heat capacity of gas and fuel	Heat capacity of solid material	Pressure
Heat transfer area with solid site	Heat transfer area with pore site	Temperature
Pressure	Temperature	Gas phase velocity
Temperature		
Fuel amount		
Initial fuel amount		
Component concentration		

* Except for this term, all other variables can be spatially distributed.

Table 2. Characteristic Parameters

Variable	Characteristic Quantity	Approximate Value
Temperature (T^*)	$\Delta_r H/C_{p,f}$	5000~16000 K
Density	ρ_f	$0.5\sim 1.5 \cdot 10^3$ Kg/m ³
Pressure	P_0	$1.01325 \cdot 10^5$ Pa
Length	L(Bond Site Length)	$5 \cdot 10^{-4}$ m
Time	L^2/D_e	$5 \cdot 10^{-3}$ s
$K_0=K_r \exp(-E_a/RT^*)$		$10\sim 1.6 \cdot 10^5$
Activation energy	E_a	$1,2\sim 1.6 \cdot 10^6$ J/mol
Diffusion coefficient	D_e	$5 \cdot 10^{-5}$ m ² /s

Table 3. Dimensionless Groups

Dimensionless group	Definition	Approximate Value
Th (Thiele modules)	$(K_0 L D_e^{-1} M_k^*)^{1/2}$	$1 \cdot 10^4 \sim 1 \cdot 10^9$
Pe	$u_0 l D_e^{-1}$	$1 \cdot 10^{-3} \sim 10$
Le	$K_f \rho_f^{-1} C_{p,f}^{-1} D_e^{-1}$	0.001~0.1
Nu	$h_s l k_s^{-1}$	0~10
$Nu_{S,L}$	$h_{L,S} l k_s^{-1}$	0~1
$Nu_{P,L}$	$h_{L,P} l k_s^{-1}$	0~1
RLSQ	$r^2 l^{-2}$	0.01~1
KKGS	$K_{p,f} k_s^{-1}$.001

Table 4. Parameters of the base case (in SI units)

Pore Site Properties	Average Value	Solid Site Properties	Average Value	Bond Site Properties	Average Value
Void volume	L^3	Volume	$1.5 \cdot L^3$	Length	$L=5 \cdot 10^{-4}$ m
Interface area for reaction	r^2	Heat transfer area between solid sites	r^2	Radius	$R=L/2$
Heat capacity of fuel	840 J kg ⁻¹ K ⁻¹	Heat capacity of solid material	840 J kg ⁻¹ K ⁻¹	Gas phase diffusivity	$5 \cdot 10^{-5}$ m ² s ⁻¹
Heat transfer area with solid site	r^2	Heat transfer area with pore site	r^2	Gas viscosity	$40 \cdot 10^{-6}$ p
Initial fuel amount	$0.5 \cdot L^3$				
Heat conductivity	0.04 w/(m K)	Heat conductivity	0.04 w/(m K)		
Nu number for heat transfer to solid site	1.0	Nu number for heat loss from pore site	0.05	Nu number for heat loss from solid site	0.05
Reaction rate coefficient				$3 \cdot 10^5$ Kg mol ⁻¹ m s ⁻¹	
Activity energy				$1.2 \cdot 10^5$ J/mol	
Heat of reaction				15000 KJ/Kg	

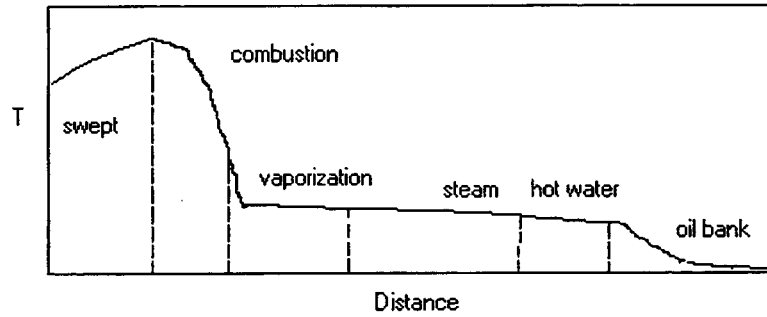
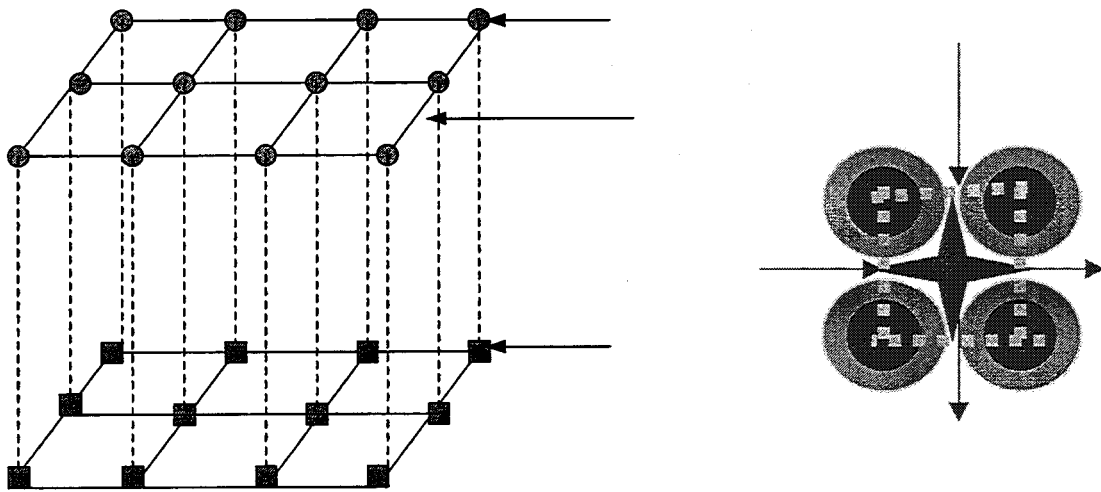


Figure 1. Schematic of Regimes in In-Situ Combustion.



B. Structure of a single pore site containing fuel

Figure 2. Structure of the pore network.

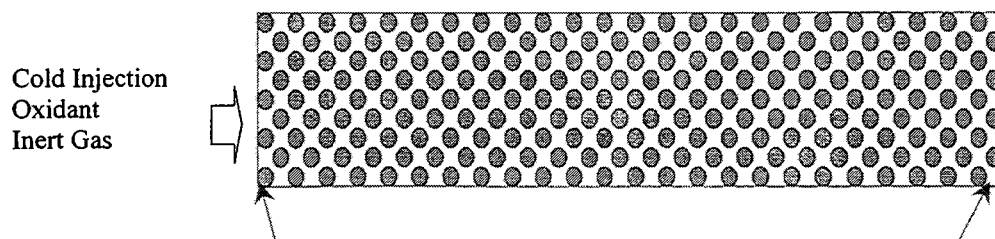
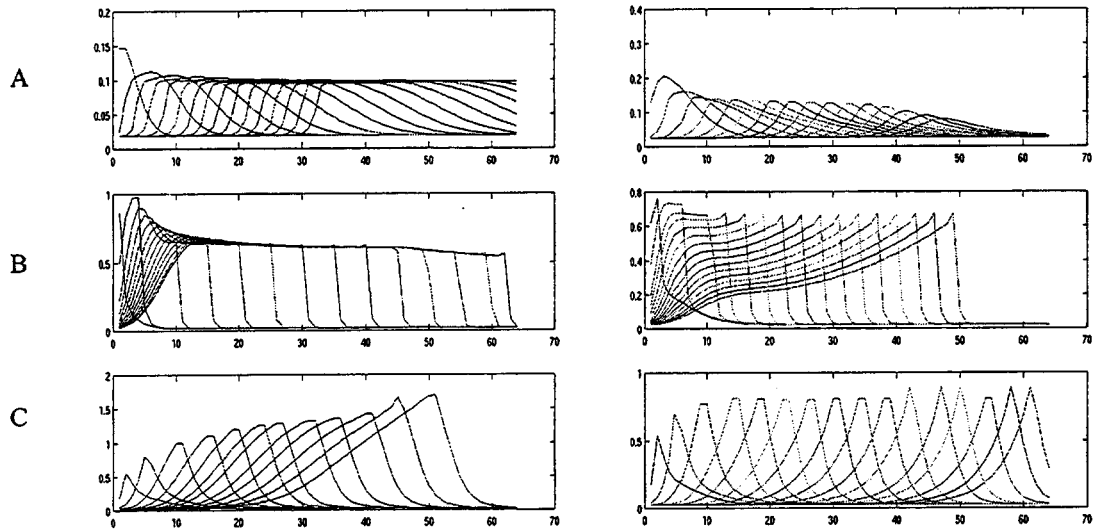


Figure 3. Sketch of the forward and reverse combustion ignition method.



A: Reaction trailing ($\delta > 1$), B: Reaction leading ($\delta < 1$), C: Maximum Accumulation ($\delta = 1$)
 Figure 4. 1-D simulation results for three different values of δ . The simulations on the right include heat losses.

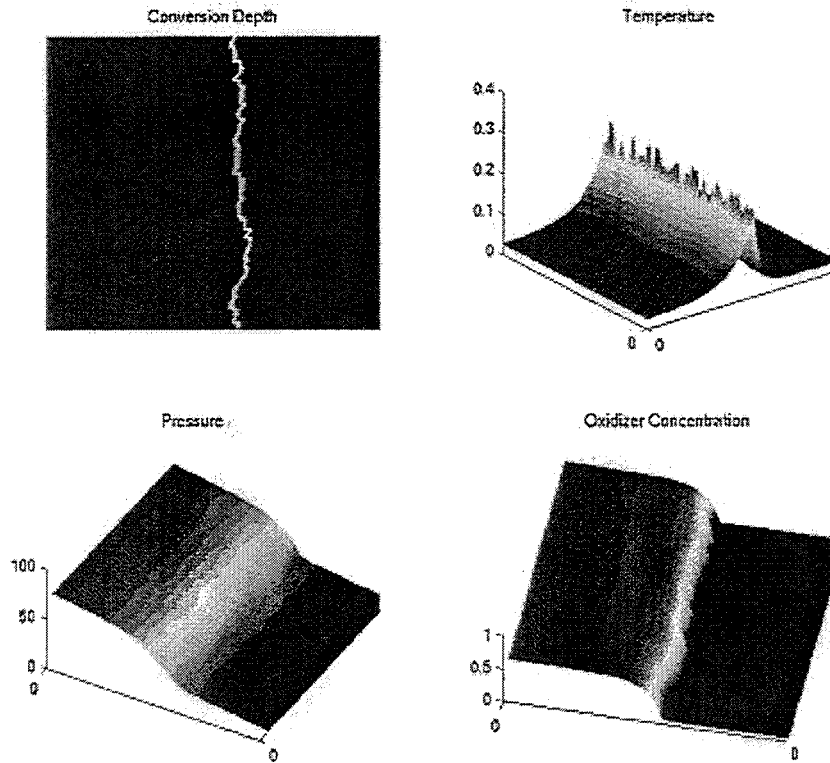


Figure 5. Patterns of forward combustion for the base case.

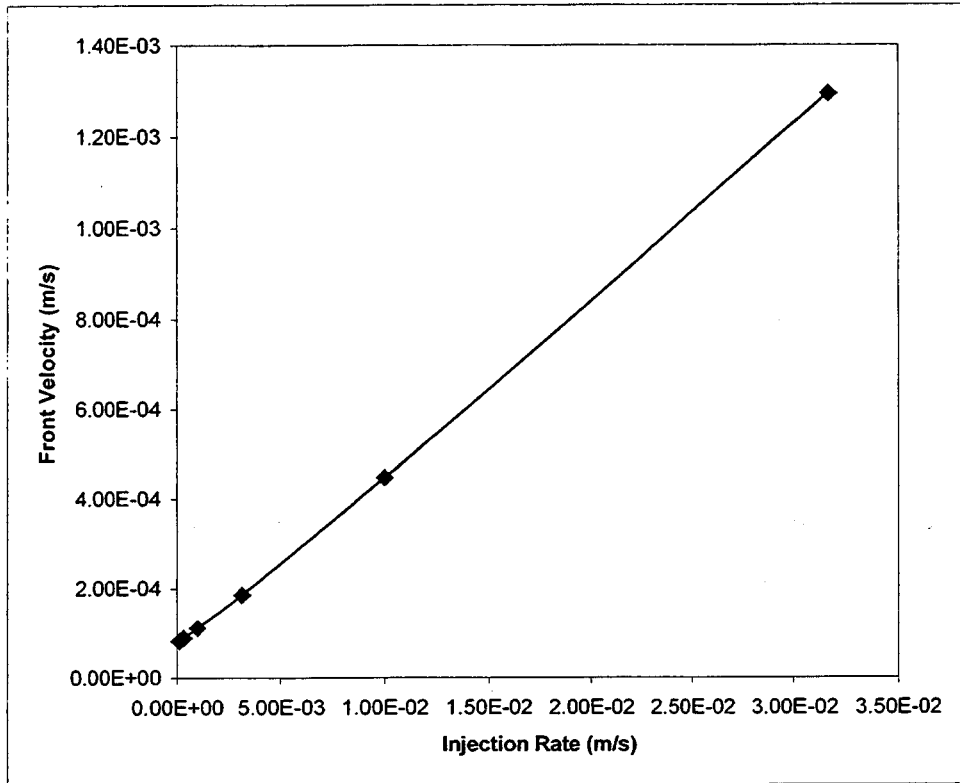


Figure 6. The steady-state front velocity as a function of the injection rate for the base-state.

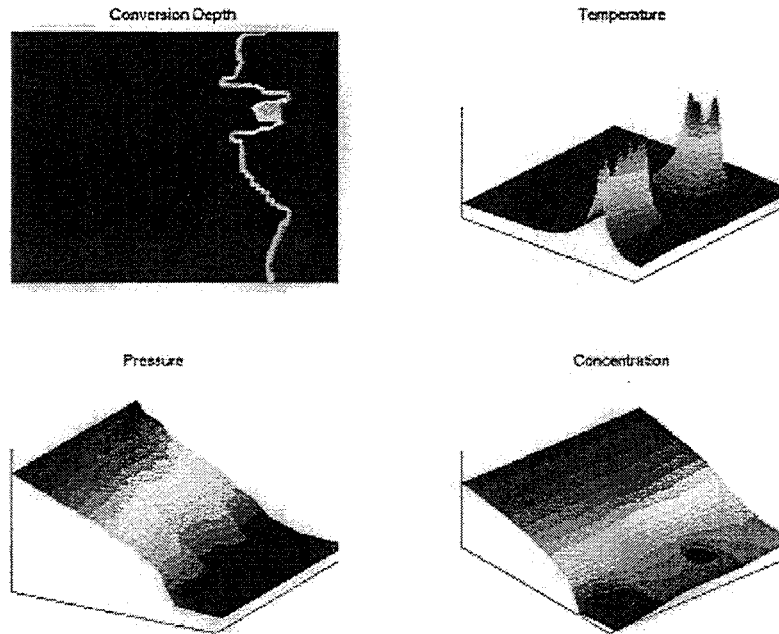


Figure 7. Patterns of forward combustion for the case of enhanced permeability in the burned region.

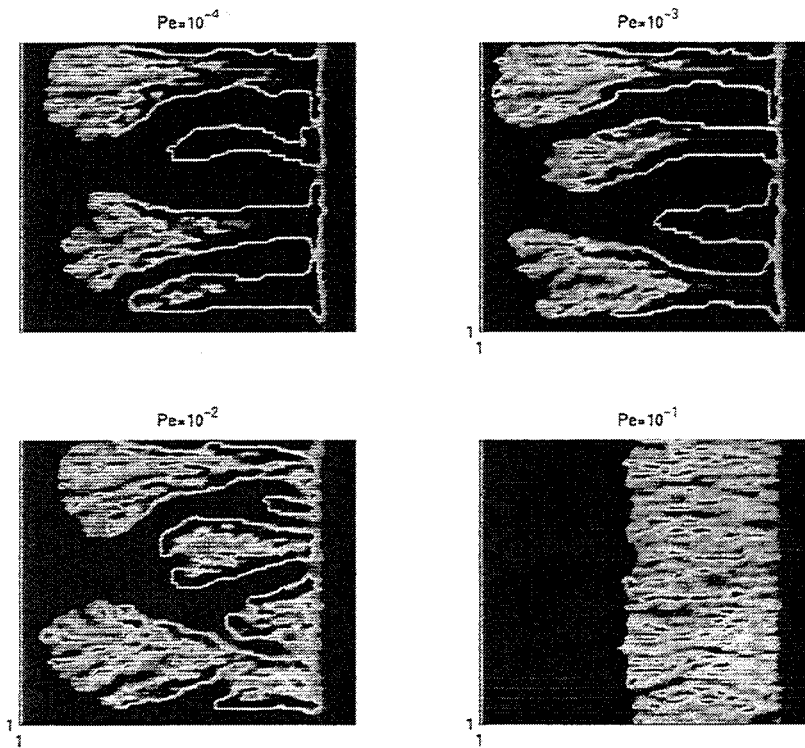


Figure 8. Conversion depth patterns for different values of the Peclet number in reverse combustion:
A) $Pe=10^{-4}$; B) $Pe=10^{-3}$; C) $Pe=10^{-2}$; D) $Pe=10^{-1}$

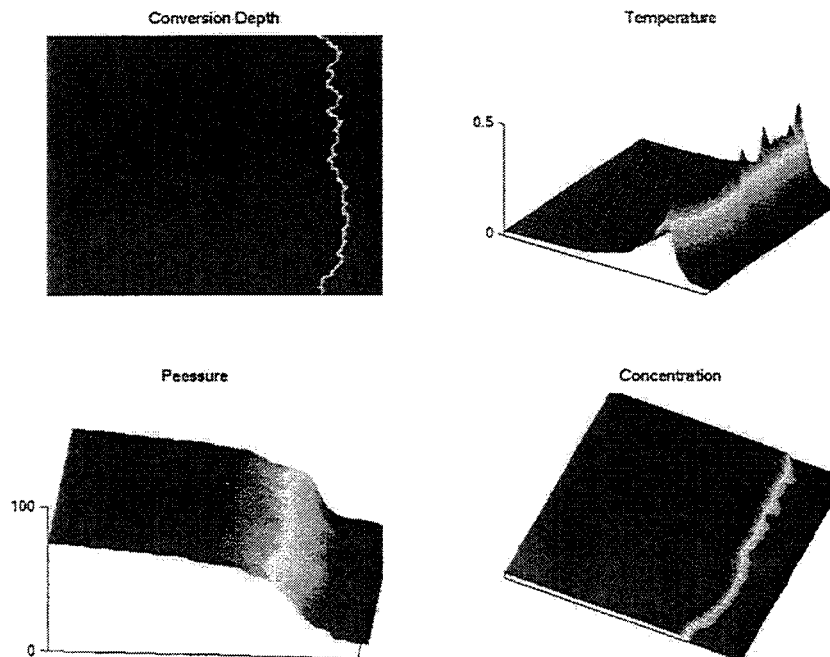


Figure 9. Patterns of forward combustion for the case of a broad pore-size distribution.

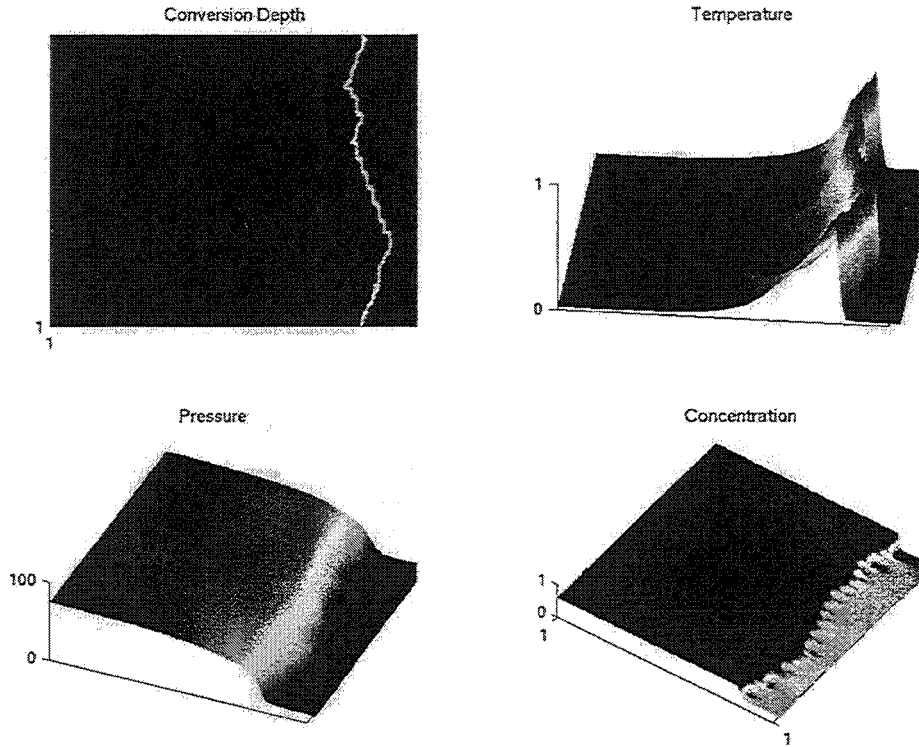


Figure 10. Patterns of forward combustion for the case of fBm pore-size distribution ($H=0.7$).

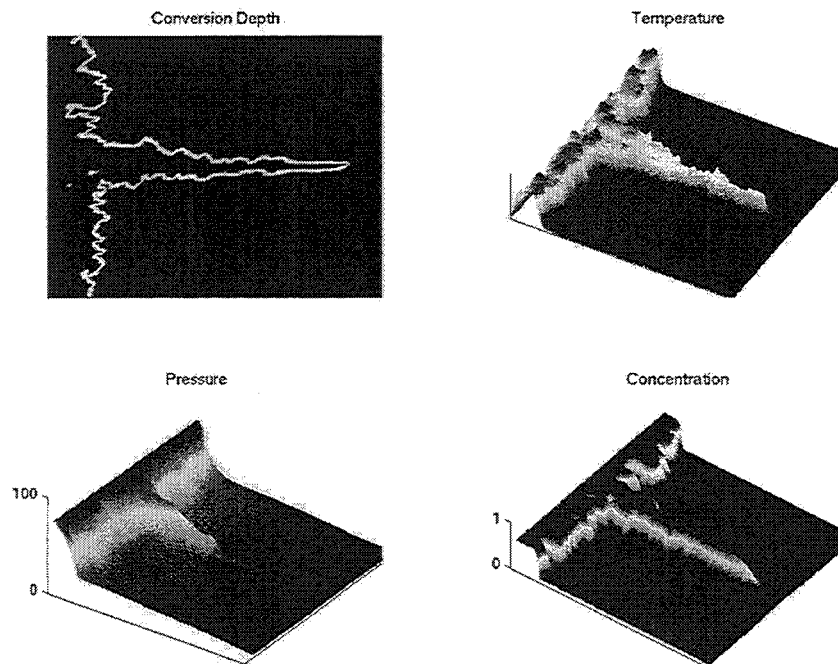


Figure 11. Patterns of forward combustion for the case of a "microfissure" in the middle of the lattice

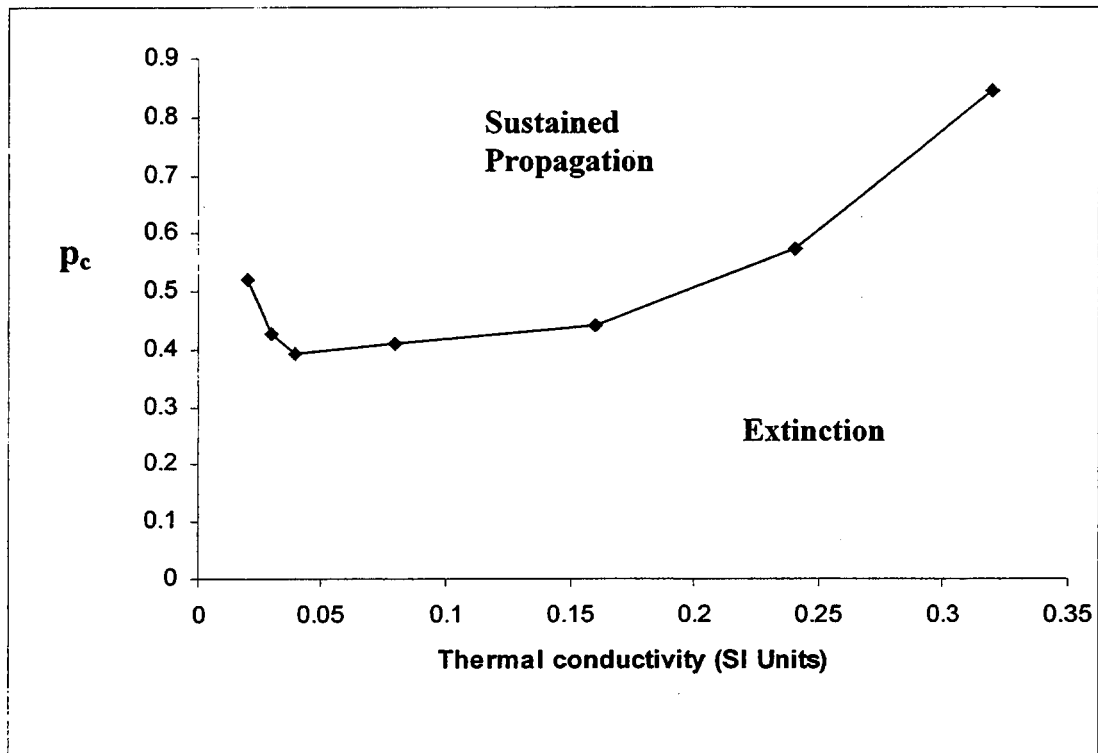


Figure 12. The percolation threshold for the onset of sustained front propagation as a function of the thermal conductivity.

